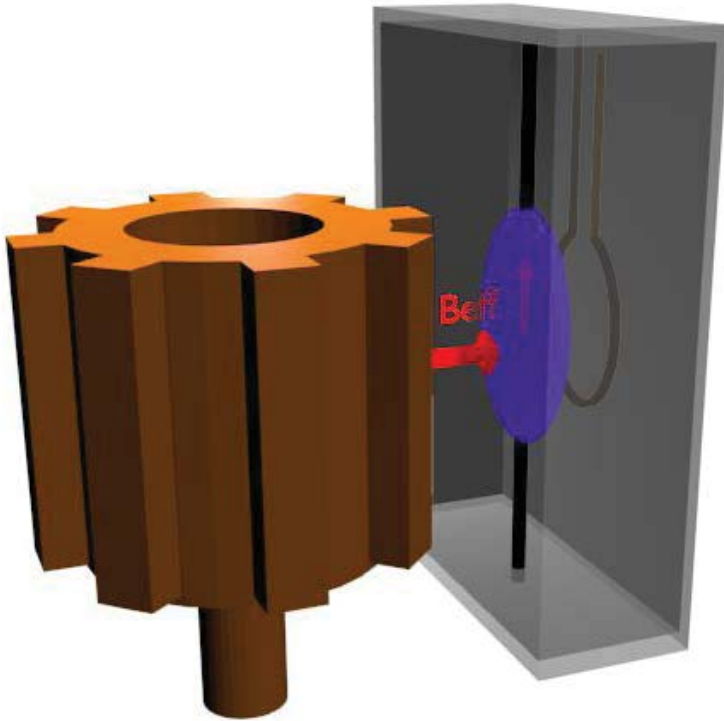


The Axion Resonant InterAction Detection Experiment (ARIADNE)



A. Geraci, UN-Reno

Light Dark World 2017, Pittsburgh

Mark Cunningham (UNR)
Mindy Harkness (UNR)
Jordan Dargert (UNR)
Chloe Lohmeyer (UNR)
Harry Fosbinder-Elkins (UNR)
Asimina Arvanitaki (Perimeter)
Aharon Kapitulnik (Stanford)
Eli Levenson-Falk (Stanford)
Sam Mumford (Stanford)
Josh Long (IU)
Chen-Yu Liu (IU)
Mike Snow (IU)
Erick Smith (IU)
Justin Shortino (IU)
Inbum Lee (IU)
Evan Weisman (IU)
Yannis Semertzidis (CAPP)
Yun Shin (CAPP)
Yong-Ho Lee (KRISS)



ibS Institute for Basic Science

University of Nevada, Reno



Geraci Lab moving January 2018



Northwestern
University

The Center for Fundamental Physics at Low Energy (CFP)

Department of Physics and Astronomy

Core Research Groups in the CFP:



[Board of Trustees Professor Gerald Gabrielse](#), one of the world's leading practitioners of fundamental, low energy physics and an active member of the National Academy of Sciences, is relocating from Harvard to Northwestern to be the founding director of the CFP. An award-winning researcher and teacher, Gabrielse has chaired both the Harvard Physics Department and the Division of Atomic, Molecular and Optical Physics (DAMOP) of the American Physical Society, and he leads the international ATRAP Collaboration at CERN. The [Gabrielse research group](#) tested the most precise prediction of the Standard Model of Particle Physics using the most precisely measured property of an elementary particle, tested the Standard Model's most fundamental symmetry to an exquisite precision, made one of the most stringent tests of Supersymmetry and other proposed improvements to the Standard Model, and started low energy antiproton and antihydrogen physics.



[Associate Professor Brian Odom](#) is joining the CFP. His fundamental physics accomplishments include a Harvard measurement of the electron magnetic moment (for which he received the DAMOP PhD thesis prize), and dark matter research done while a Kavli postdoctoral fellow at the University of Chicago. The [Odom research group](#) at Northwestern is successfully developing methods to trap, cool and probe molecular ions. One motivation is to use these for fundamental physics measurements, including new searches for time variations of some of the fundamental constants of nature.

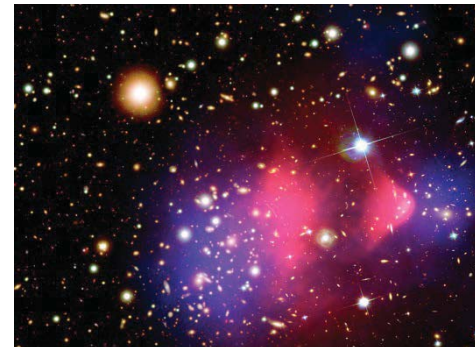
Two new faculty members will shortly be hired to lead additional core research groups of the CFP.

Opportunities for postdocs, students!
New faculty search underway Fall 2017!

Axions

- Light pseudoscalar particles in many theories
Beyond Standard model
- Peccei-Quinn Axion (QCD) solves strong CP problem $\theta_{QCD} < 10^{-10}$
- Dark matter candidate

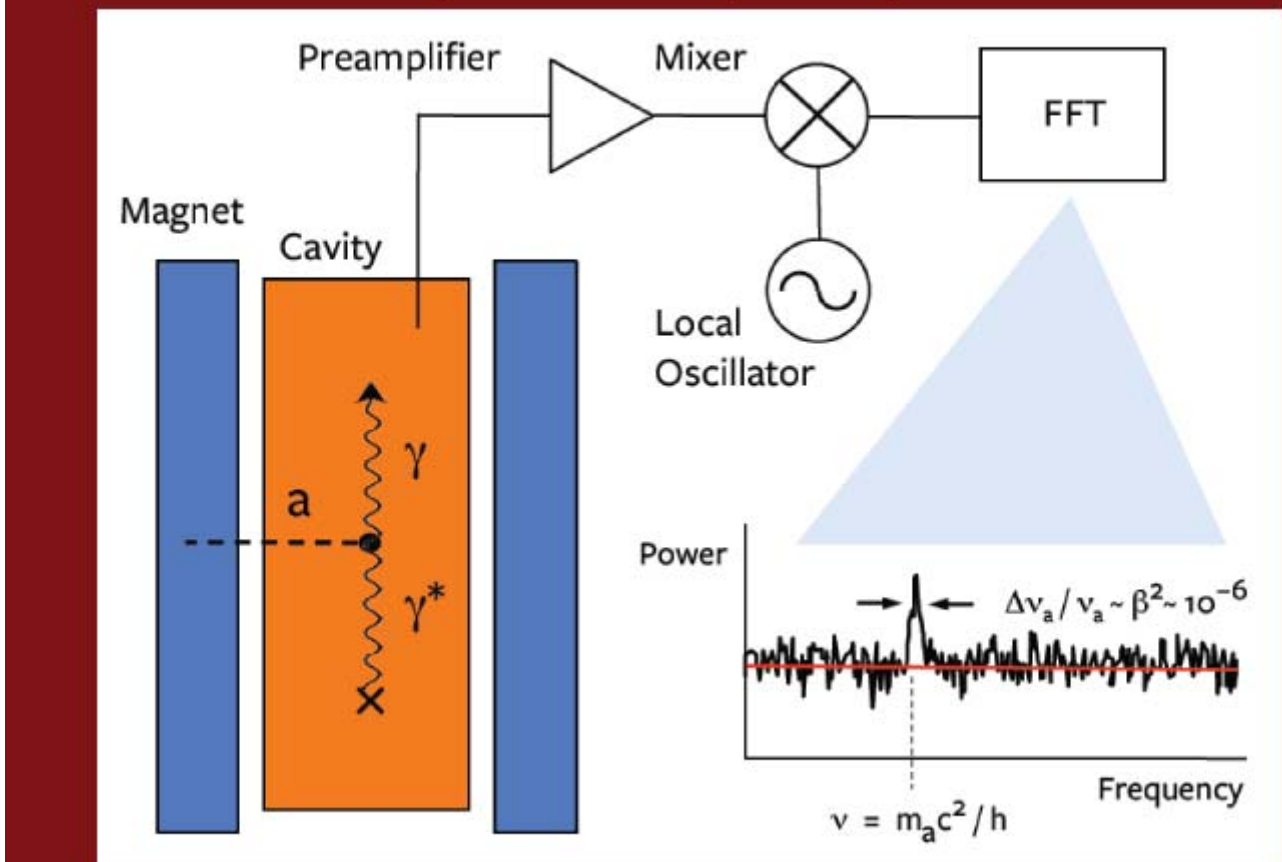
Experiments: e.g. ADMX, HAYSTACK, LC-circuit,
Casper



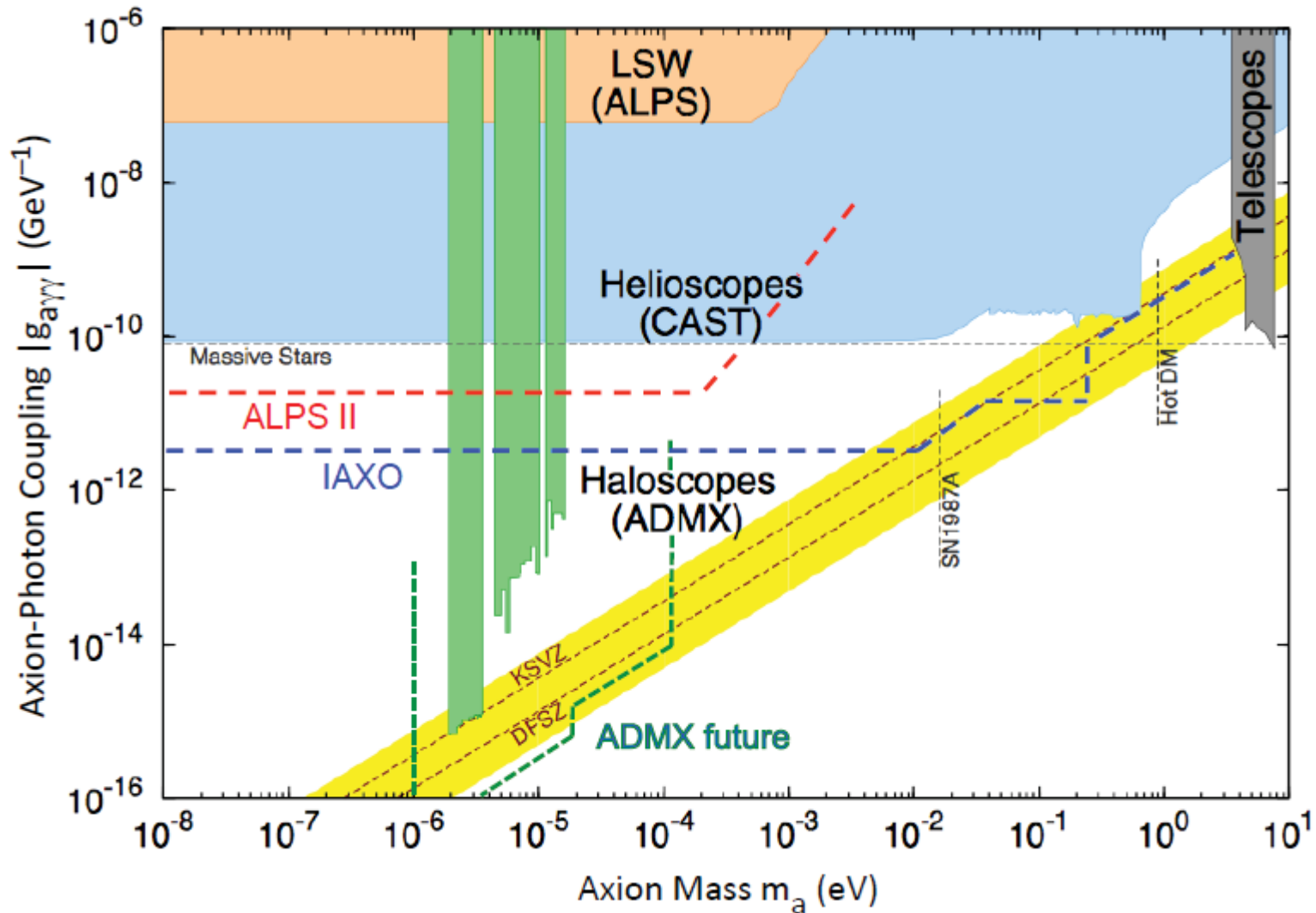
- R. D. Peccei and H. R. Quinn, Phys. Rev. Lett. 38, 1440 (1977);
- S. Weinberg, Phys. Rev. Lett. 40, 223 (1978);
- F. Wilczek, Phys. Rev. Lett. 40, 279 (1978).
- J. E. Moody and F. Wilczek, Phys. Rev. D 30, 130 (1984).

Haloscopes

The principle of the microwave-cavity haloscopes:
ADMX, ADMX-HF, CAPP, ORGAN



Axion Parameter space



Adapted from Graham, arxiv: 1602.00039

Axion couplings

$$\frac{a}{f_a} F_{\mu\nu} \tilde{F}^{\mu\nu}$$



Coupling to electromagnetic field
ADMX, DM Radio, LC Circuit

$$\frac{a}{f_a} G_{\mu\nu} \tilde{G}^{\mu\nu}$$

Coupling to gluon field

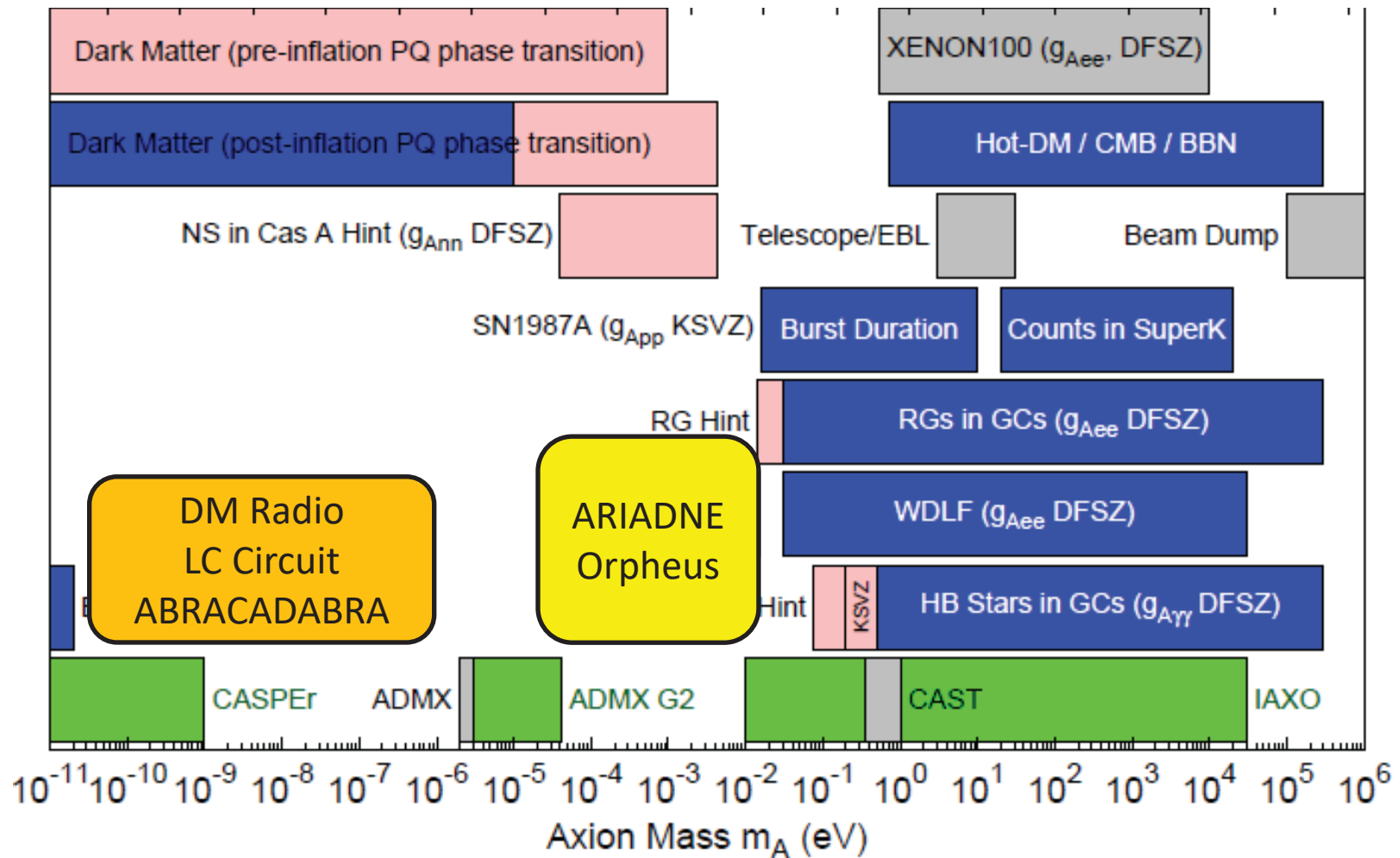
e.g. **CASPER-electric**

$$\frac{\partial_\mu a}{f_a} \bar{\Psi}_f \gamma^\mu \gamma_5 \Psi_f$$

Coupling to fermions

e.g. **CASPER-wind, QUAX**

QCD Axion parameter space



Adapted from <http://pdg.lbl.gov/2015/reviews/rpp2015-rev-axions.pdf>

Axion and ALP searches

Source	Coupling	
Photons	Nucleons	
Dark Matter (Cosmic) axions	ADMX, HAYSTACK, DM Radio, LC Circuit, ABRACADABRA	CASPER
Solar axions	CAST IAXO	
Lab-produced axions	Light-shining-thru- walls (ALPS, ALPS-II)	ARIADNE

Axion-exchange between nucleons

- Scalar coupling $\propto \theta_{QCD}$

$$\mathcal{L} \supset \frac{\theta_{QCD}}{f_a} \mu a \bar{\psi} \psi$$

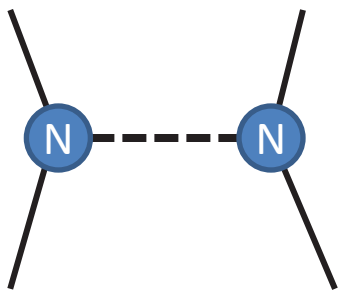
- Pseudoscalar coupling

$$\mathcal{L} \supset \frac{\partial_\mu a}{f_a} \bar{\psi} \gamma_\mu \gamma_5 \psi$$

In the non-relativistic limit:

$$\mathcal{L} \supset \frac{\vec{\nabla}_a}{f_a} \cdot \vec{\sigma}$$

Axion acts a force mediator between nucleons



$$(g_s^N)^2$$

Monopole-monopole

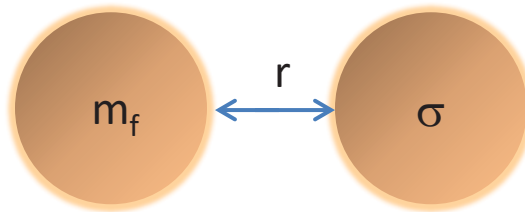
$$g_s^N g_P^N$$

Monopole-dipole

$$(g_p^N)^2$$

dipole-dipole

Spin-dependent forces



Monopole-Dipole axion exchange

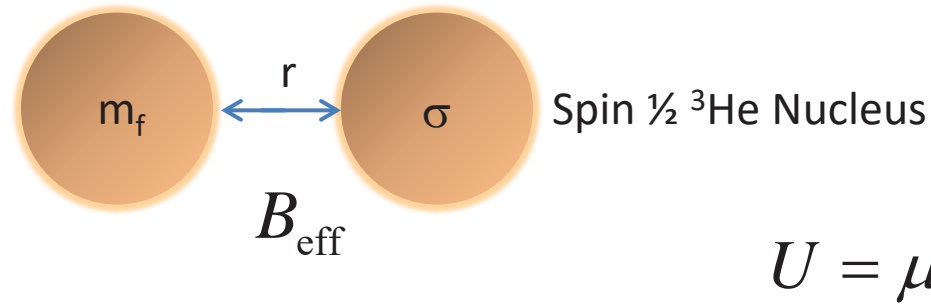
$$U(r) = \frac{\hbar^2 g_s^N g_p^N}{8\pi m_f} \left(\frac{1}{r\lambda_a} + \frac{1}{r^2} \right) e^{-r/\lambda_a} (\hat{\sigma} \cdot \hat{r}) \equiv \mu \cdot B_{\text{eff}}$$

$$m_a < 6 \text{ meV} \quad \longrightarrow \quad \lambda_a > 30 \text{ } \mu\text{m}$$

Fictitious magnetic field

- Different than ordinary B field
- Does not couple to angular momentum
- Unaffected by magnetic shielding

Using NMR for detection



Bloch Equations

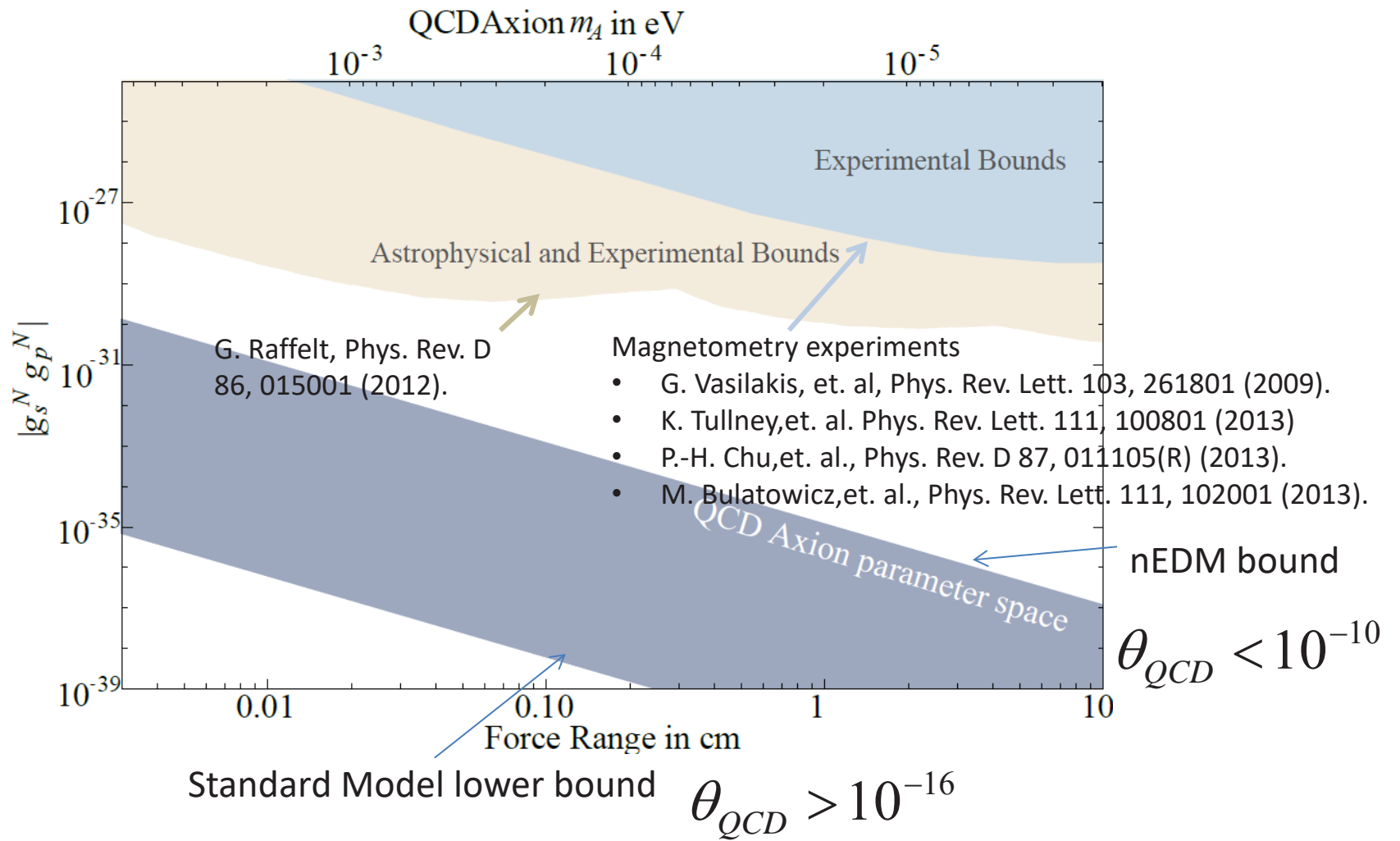
$$\frac{d\vec{M}}{dt} = \gamma \vec{M} \times \vec{B}$$

$$\begin{array}{c} \hline | \uparrow \rangle \\ \omega = \frac{2\mu_N \cdot B_{\text{ext}}}{\hbar} \\ \hline | \downarrow \rangle \end{array}$$

Spin precesses at nuclear spin Larmor frequency $\omega = \gamma B$

Axion B_{eff} modifies measured Larmor frequency

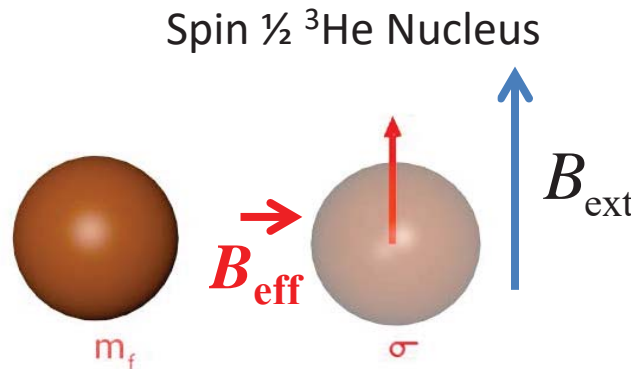
Constraints on spin dependent forces



ARIADNE: uses resonant enhancement

Oscillate the mass at
Larmor frequency

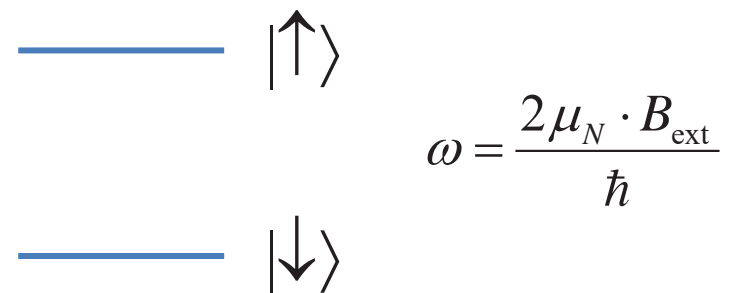
$$B_{\text{eff}} = B_{\perp} \cos(\omega t)$$



$$U = \mu \cdot B_{\text{ext}}$$

Bloch Equations

$$\frac{d\vec{M}}{dt} = \gamma \vec{M} \times \vec{B}$$



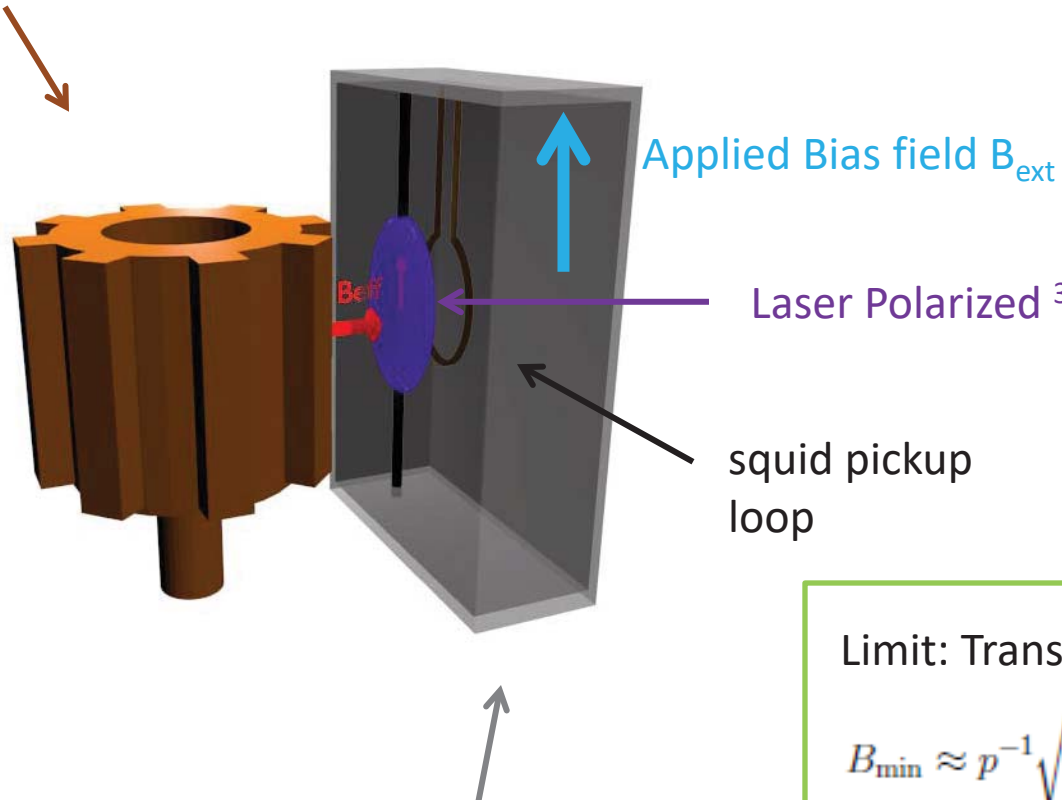
Time varying Axion B_{eff} drives spin precession
→ produces transverse magnetization

Amplitude is resonantly enhanced
by Q factor $\sim \omega T_2$.

Can be detected with a SQUID

Concept for ARIADNE

Unpolarized (tungsten) segmented cylinder sources B_{eff}



$$\omega = \frac{2\mu_N \cdot B_{\text{ext}}}{\hbar}$$

Laser Polarized ³He gas senses B_{eff} (Indiana U)



Limit: Transverse spin projection noise

$$B_{\min} \approx p^{-1} \sqrt{\frac{2\hbar}{n_s \mu_{^3\text{He}} \gamma V T_2}} = 10^{-20} \frac{T}{\sqrt{\text{Hz}}} \times \\ \left(\frac{1}{p}\right) \left(\frac{1 \text{ cm}^3}{V}\right)^{1/2} \left(\frac{10^{21} \text{ cm}^{-3}}{n_s}\right)^{1/2} \left(\frac{1000 \text{ sec}}{T_2}\right)^{1/2}$$

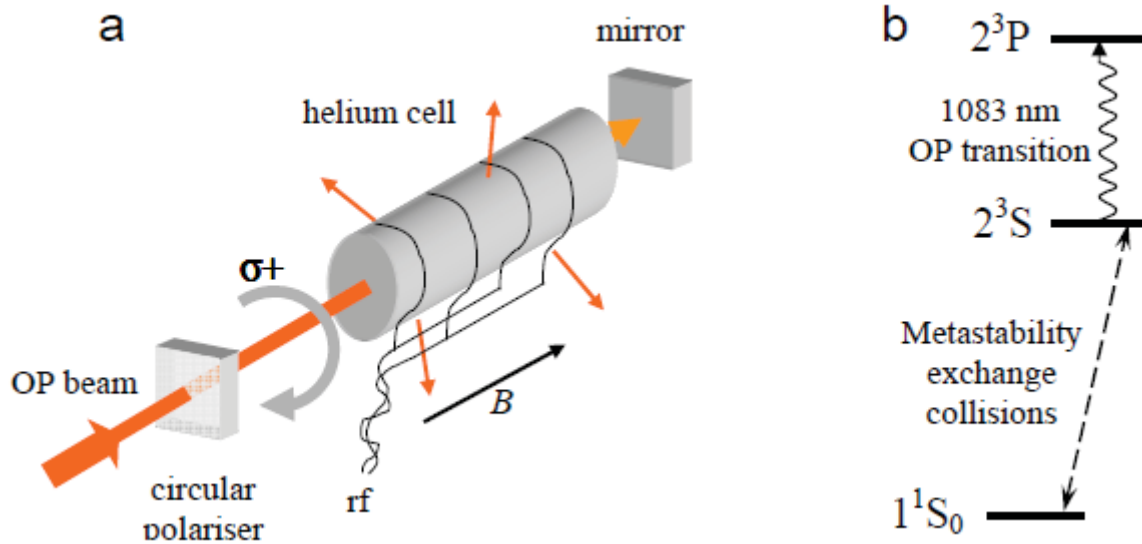
Hyperpolarized ^3He

- Ordinary magnetic fields cannot be used to reach near unity polarization

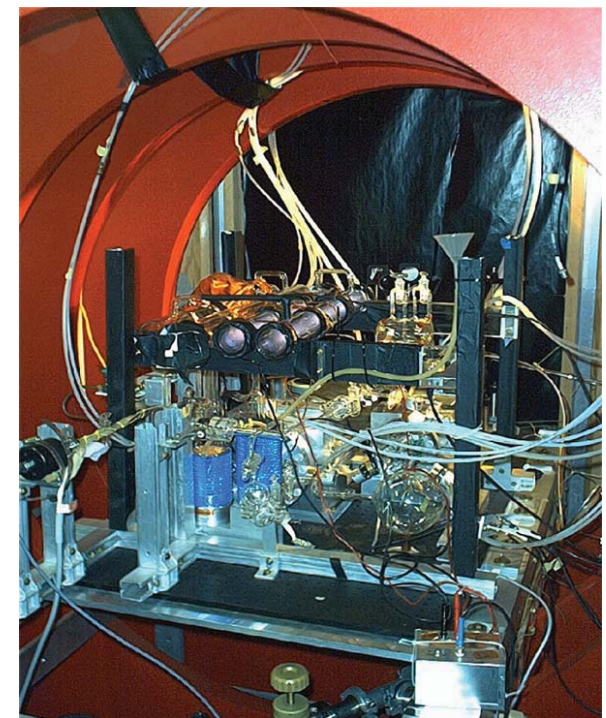
$$\exp[-\mu_N B / k_B T]$$

Optical pumping techniques

- Metastability exchange optical pumping

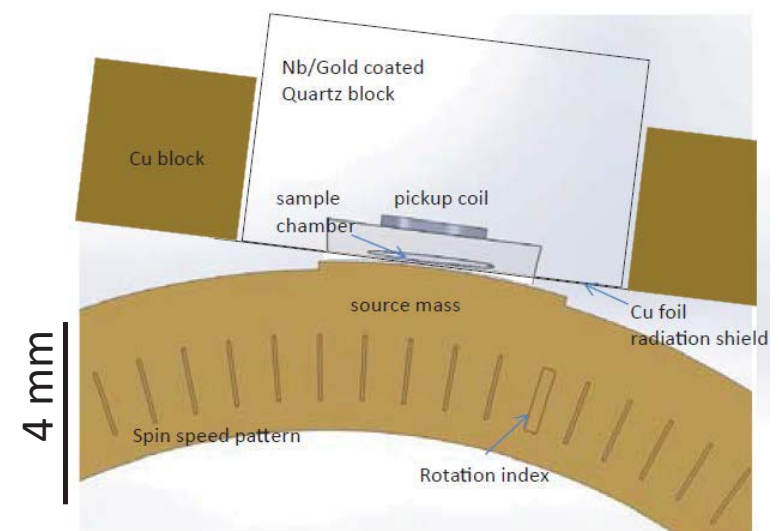
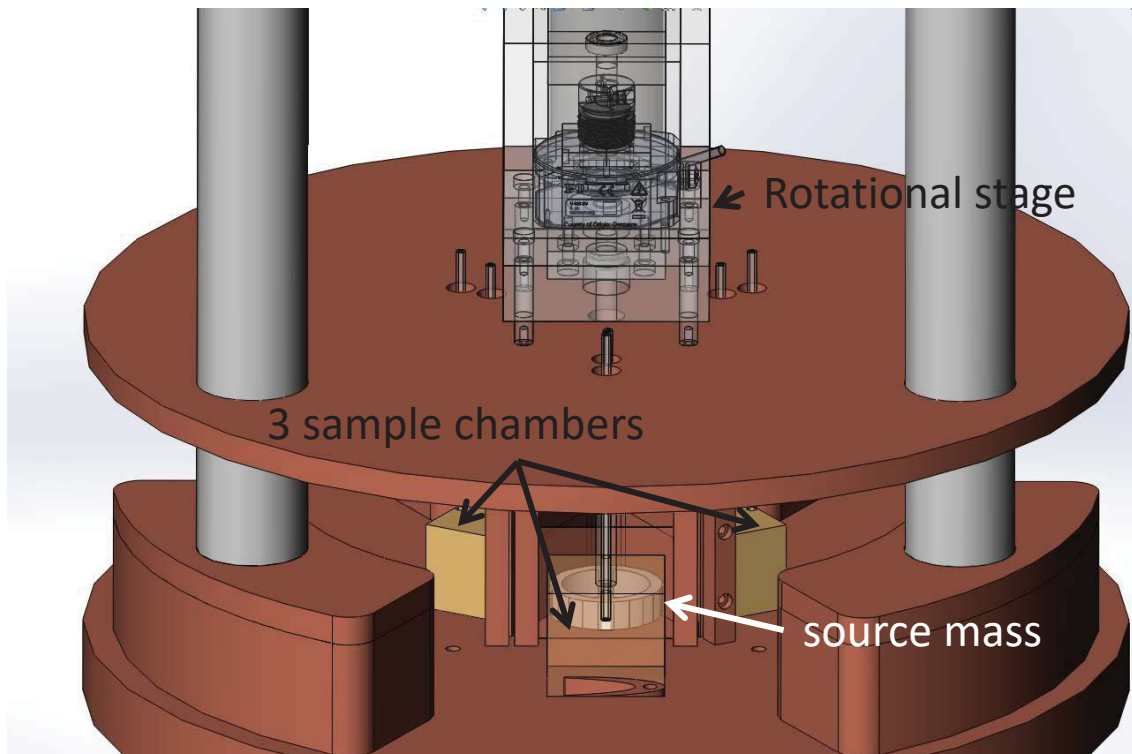


Indiana U. MEOP apparatus



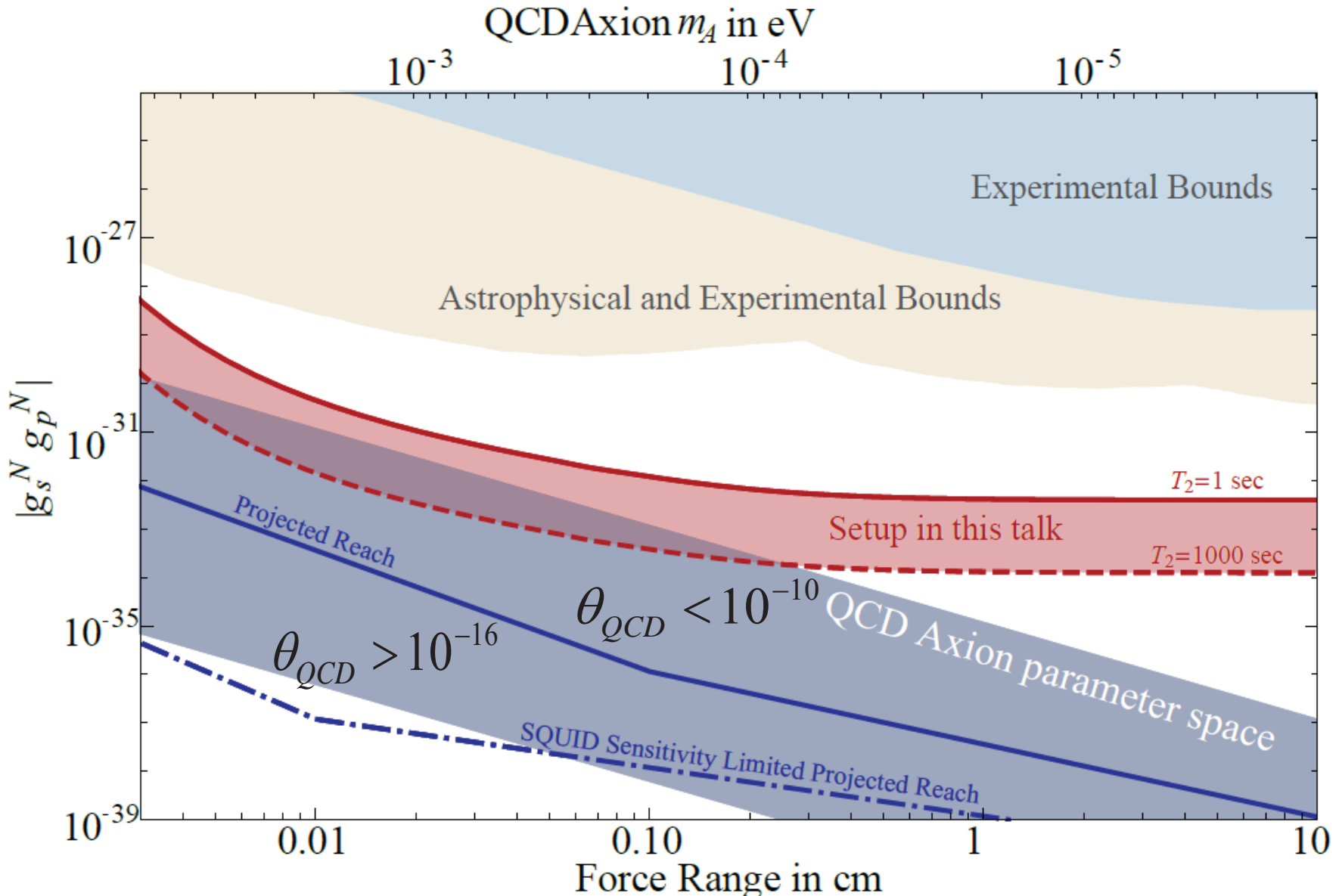
Rev. Sci. Instrum. 76, 053503 (2005)

Experimental parameters

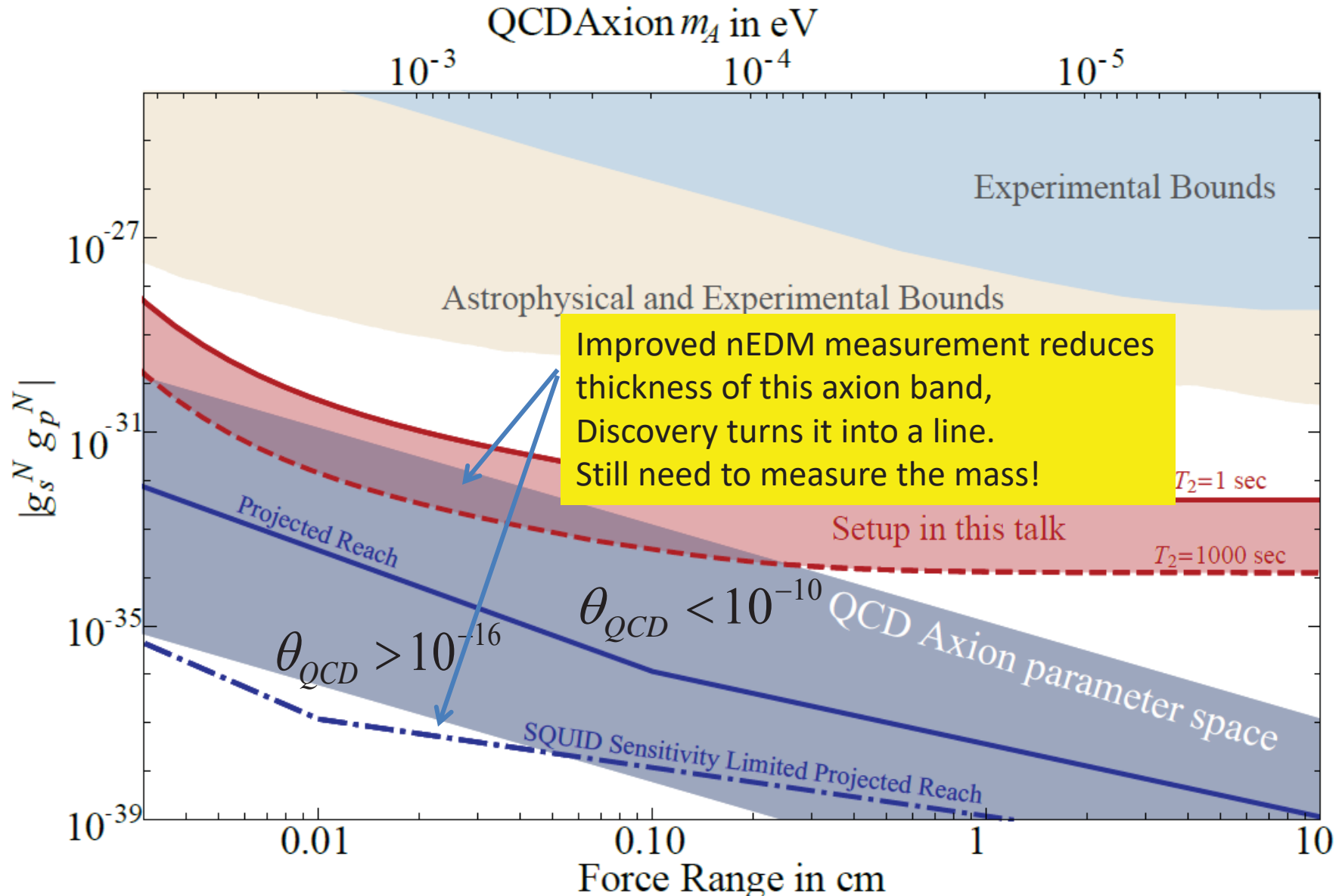


11 segments
100 Hz nuclear spin precession frequency
 $2 \times 10^{21} / \text{cc}$ ^3He density
10 mm x 3 mm x 150 μm volume
Separation 200 μm
Tungsten source mass (high nucleon density)

Sensitivity



Complementarity with nEDM experiments



Experimental challenges

Systematic Effect/Noise source	Background Level	Notes
Magnetic gradients	$3 \times 10^{-6} \text{ T/m}$	Limits T_2 to $\sim 100 \text{ s}$
Vibration of mass	10^{-22} T	Possible to improve w/shield geometry
External vibrations	$5 \times 10^{-20} \text{ T}/\sqrt{\text{Hz}}$	For $10 \mu\text{m}$ mass wobble at ω_{rot}
Patch Effect	$10^{-21} \left(\frac{V_{\text{patch}}}{0.1V} \right)^2 \text{ T}$	For $1 \mu\text{m}$ sample vibration (100 Hz)
Flux noise in squid loop	$2 \times 10^{-20} \text{ T}/\sqrt{\text{Hz}}$	Can reduce with V applied to Cu foil
Trapped flux noise in shield	$7 \times 10^{-20} \frac{\text{T}}{\sqrt{\text{Hz}}}$	Assuming $1\mu\Phi_0/\sqrt{\text{Hz}}$
Johnson noise	$10^{-20} \left(\frac{10^8}{f} \right) \text{ T}/\sqrt{\text{Hz}}$	Assuming 10 cm^{-2} flux density
Barnett Effect	$10^{-22} \left(\frac{10^8}{f} \right) \text{ T}$	f is SC shield factor (100 Hz)
Magnetic Impurities in Mass	$10^{-25} - 10^{-17} \left(\frac{\eta}{1\text{ppm}} \right) \left(\frac{10^8}{f} \right) \text{ T}$	Can be used for calibration above 10 K
Mass Magnetic Susceptibility	$10^{-22} \left(\frac{10}{f} \right) \text{ T}$	η is impurity fraction (see text)
		Assuming background field is 10^{-10} T
		Background field can be larger if $f > 10^8$

Table 1: Table of estimated systematic error and noise sources, as discussed in the text. The projected sensitivity of the device is $3 \times 10^{-19} \left(\frac{1000\text{s}}{T_2} \right) \text{ T}/\sqrt{\text{Hz}}$

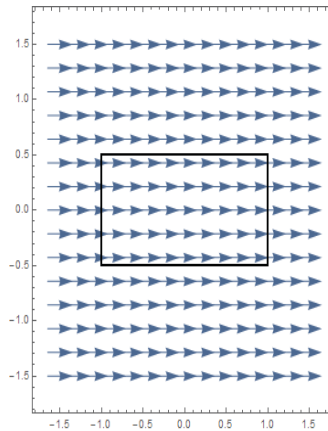
- Design/Simulation Work: Magnetic gradient reduction strategy
- Experimental testing in progress: Vibration tests, Shielding factor f test thin-film SC

Superconducting Magnetic Shielding

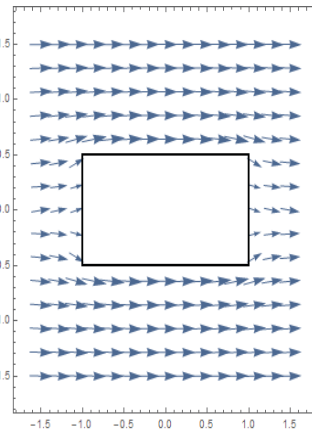
→ Essential to avoid Johnson noise

Meissner Effect

- No magnetic flux across superconducting boundary



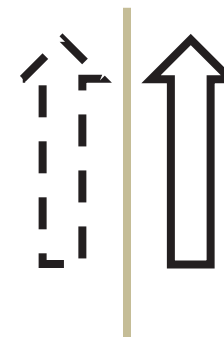
$T > T_c$



$T < T_c$

Method of Images

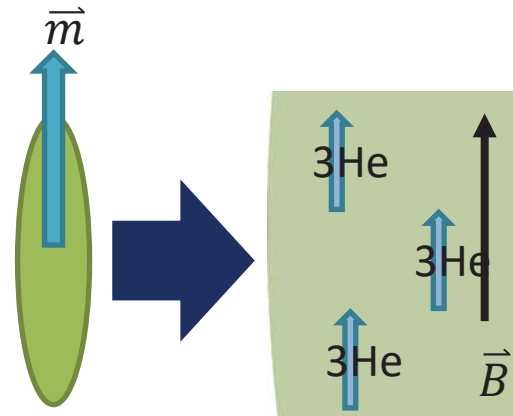
- Make “image currents” mirrored across the superconducting boundary



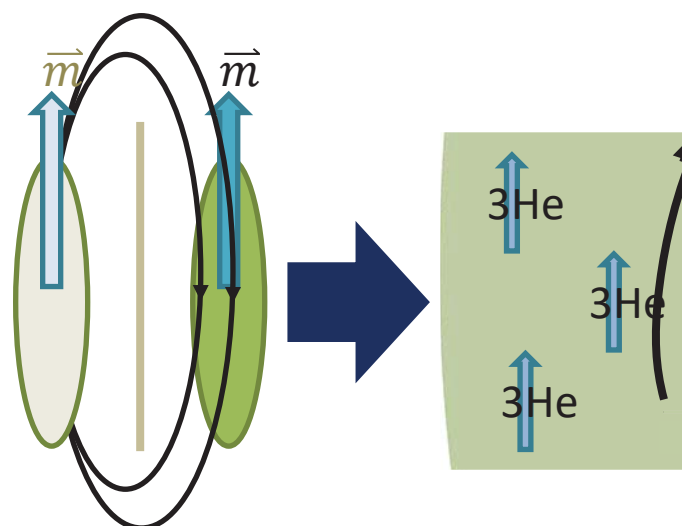
Dipole with image

The Problem of Unwanted Images

- ARIADNE uses magnetized spheroid
 - Constant interior field



- Magnetic shielding introduces “image spheroid”
 - Interior field varies
- variations in nuclear Larmor frequency



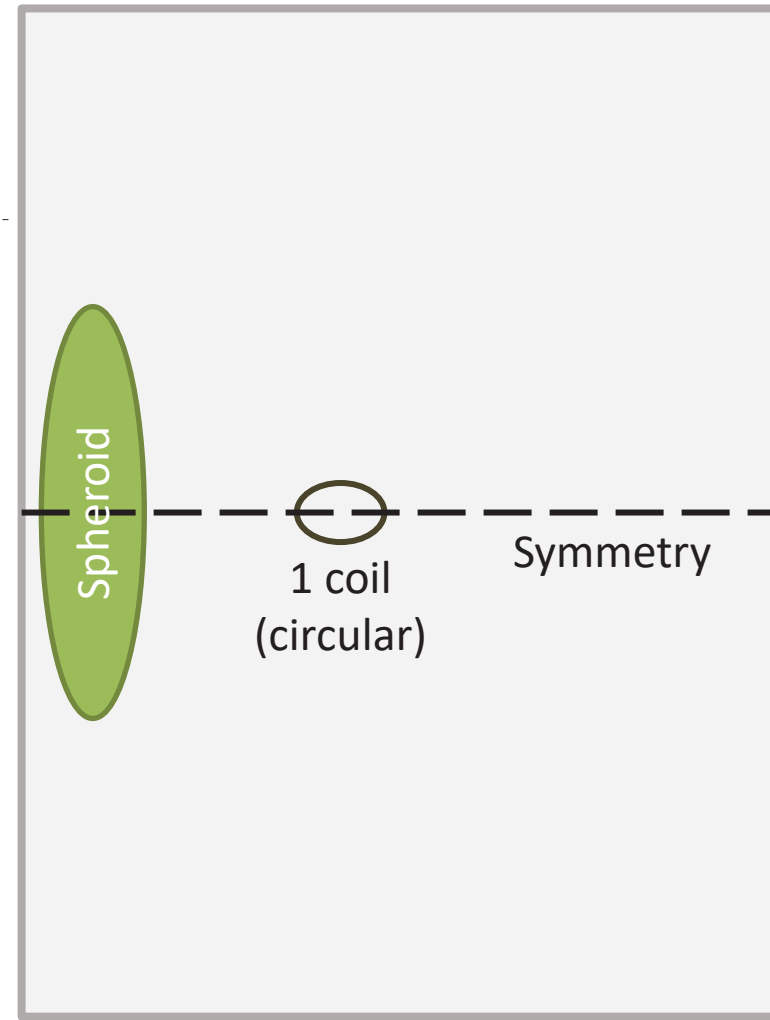
- $B_{in} = \text{const.}$
- $\frac{\vec{B}_{in}}{B_{in}} \parallel \vec{m}_i$

- $B_{in} \neq \text{const.}$
- $\frac{\vec{B}_{in}}{B_{in}} \nparallel \vec{m}_i$

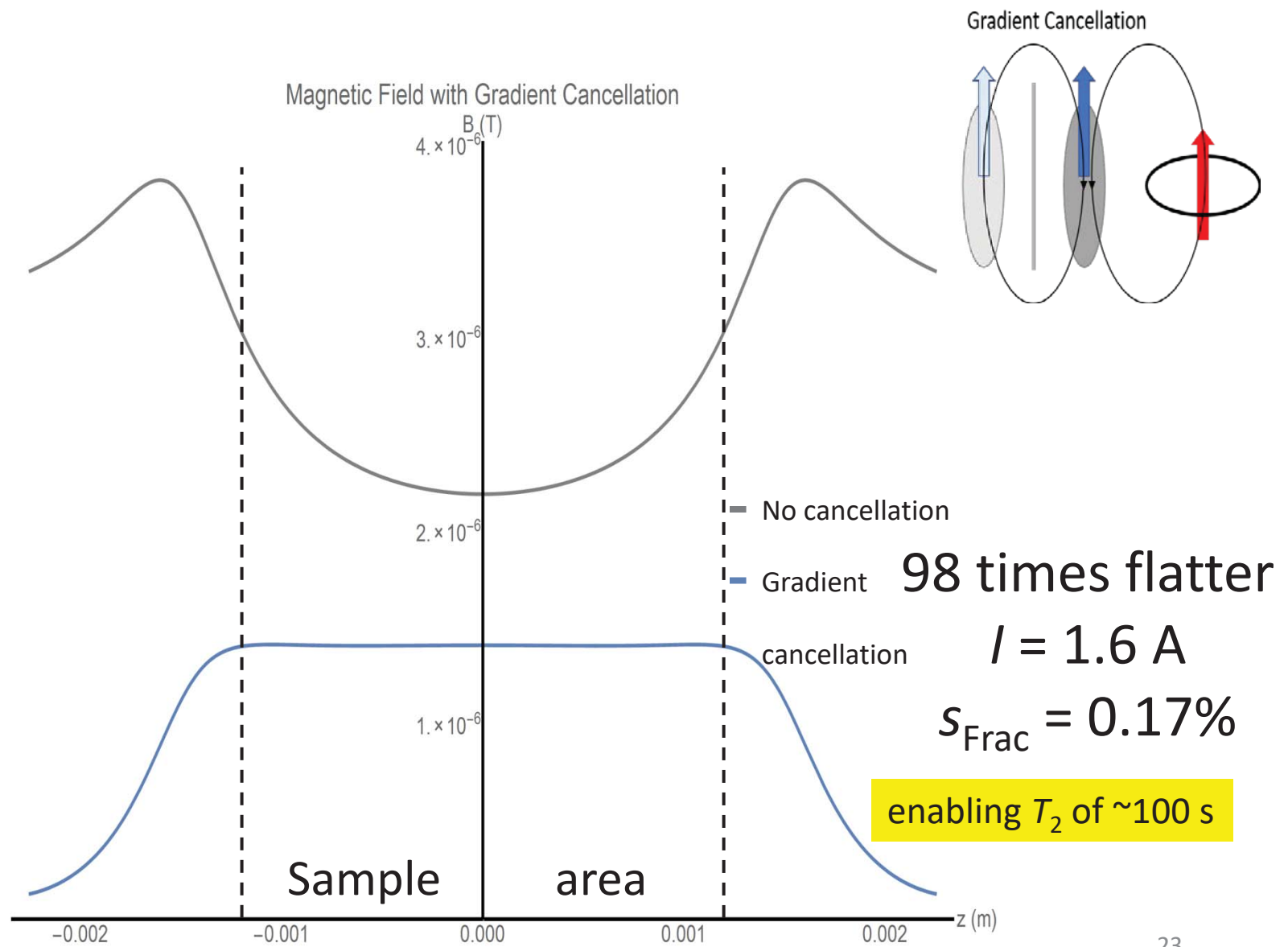
But want to drive entire sample on resonance

Flattening Solution

- 1 coil – simple configuration
- Expected field from spheroid $\sim 1 \mu\text{T}$
 - I on the 0.1 – 1 A range

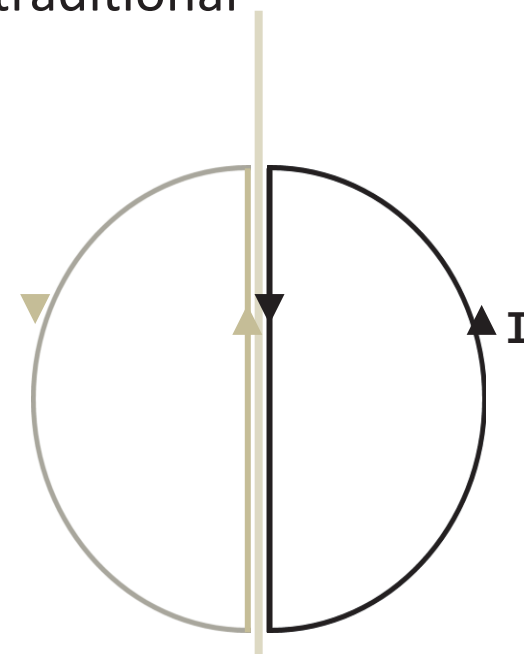


Gradient Cancellation

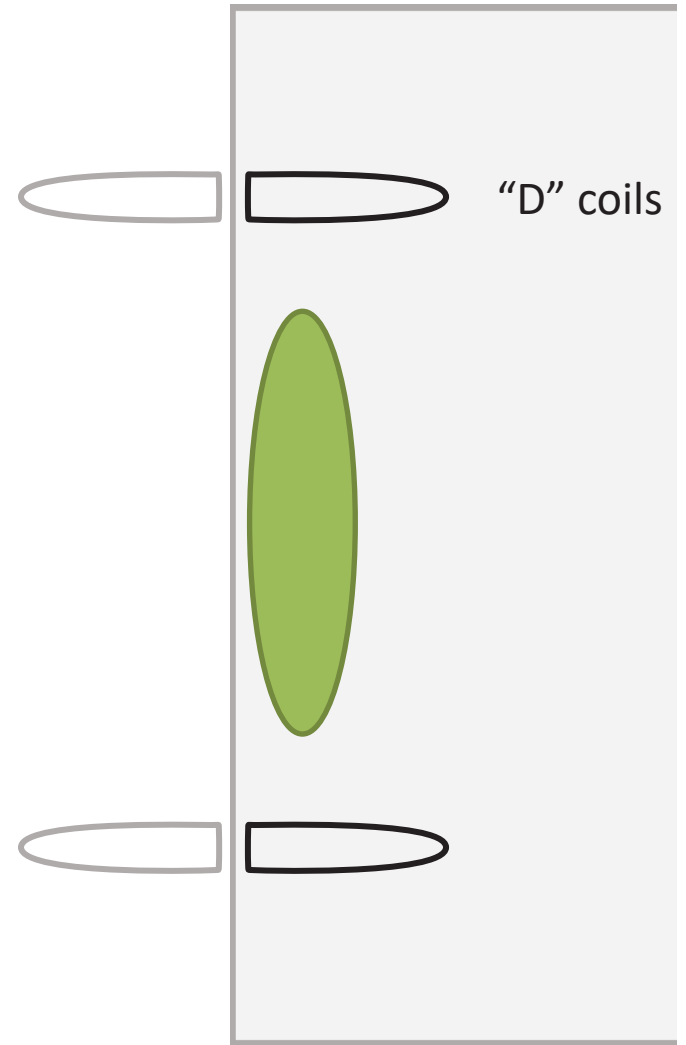


Tuning Solution – “D” Coils

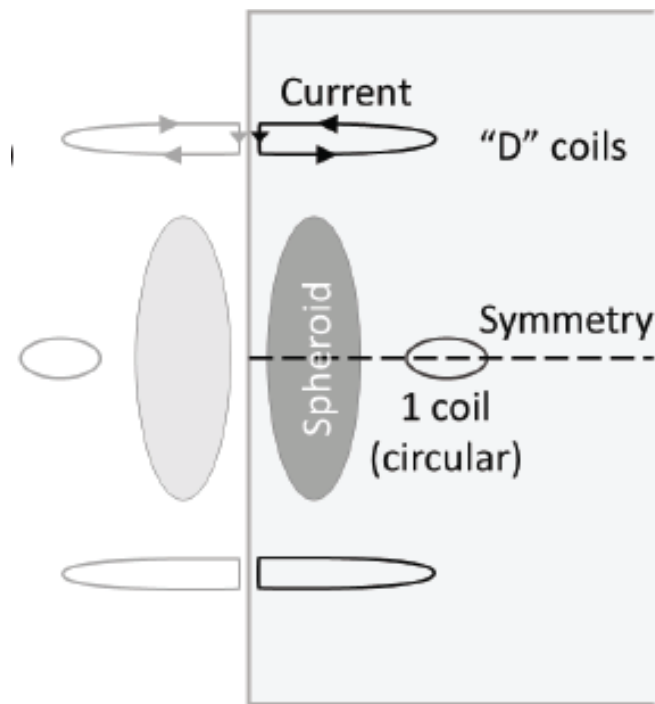
- Tune field with Helmholtz coils
 - Helmholtz field only flat near the center
 - Geometry restrictions prevent the spheroid from being centered in traditional Helmholtz coils
- “D” coils look like Helmholtz coils when their images are included
- Inner straight-line currents cancel
- Outer currents do not



One “D” coil and image (bird’s eye view)



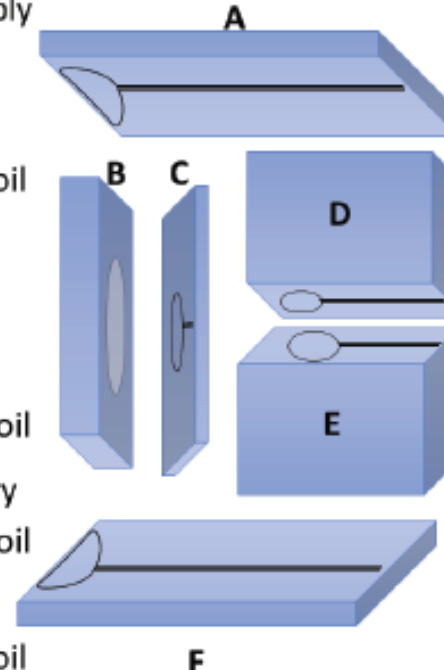
Quartz block assembly



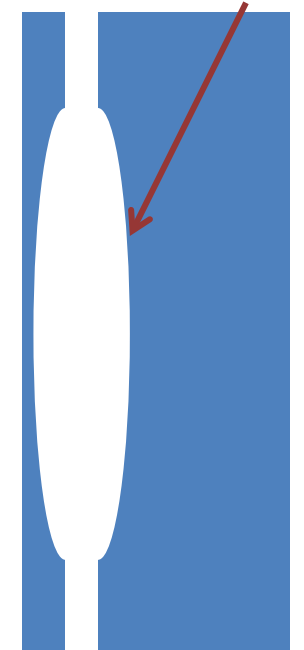
Block Assembly

Key:

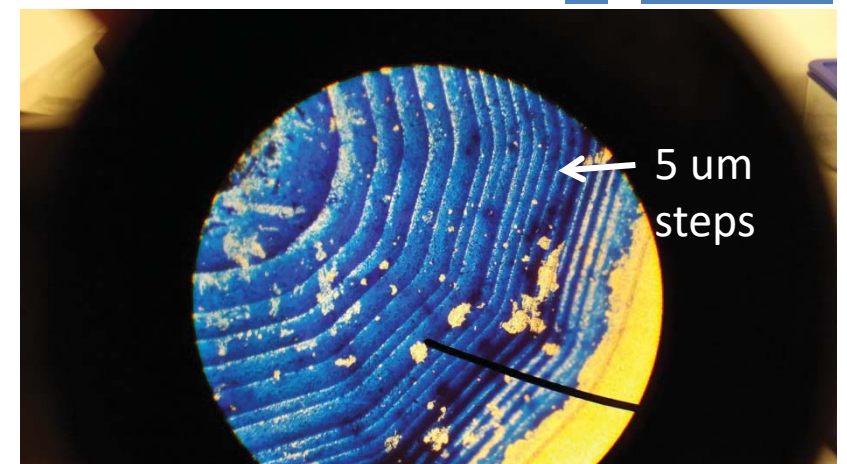
- A – Upper Helmholtz Coil
- B – Spheroid
- C – SQUID
- D – Primary Correction Coil
- E – Secondary Correction Coil
- F – Lower Helmholtz Coil



Spheriodal pocket



Milled spheriodal pocket in quartz



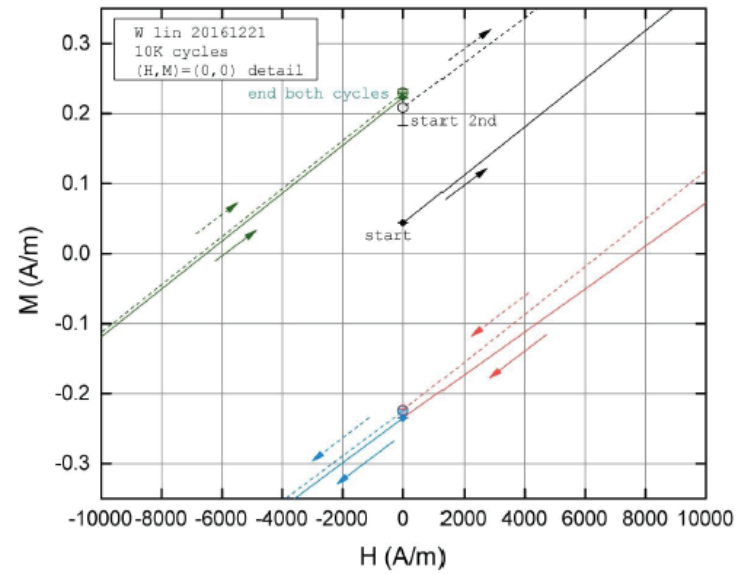
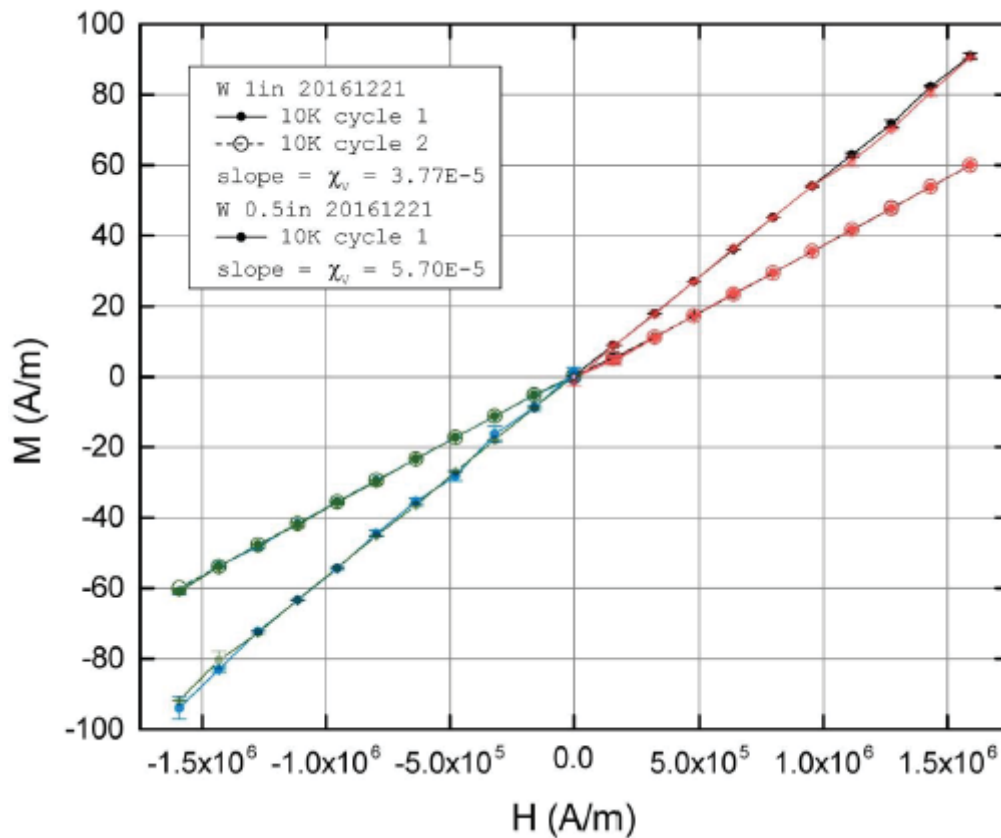
Fabrication/polishing tests is process – Oct 2017

Tungsten Source Mass Prototype

11 segments, 3.8 cm diameter Tungsten
Sprocket prototype, Wire EDM

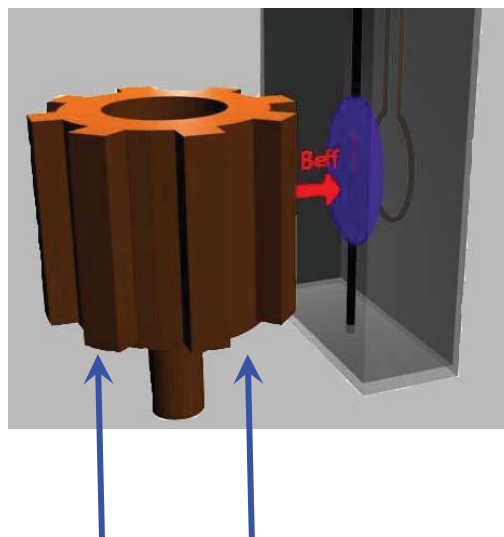
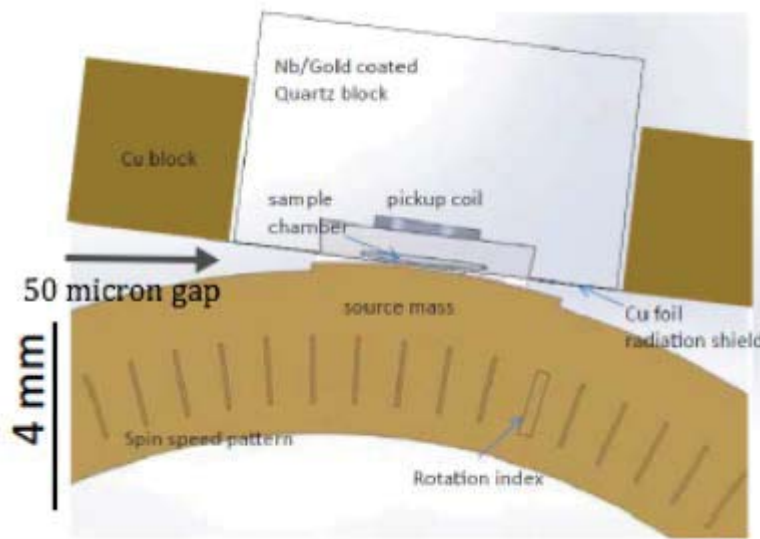


Magnetic impurity testing in Tungsten
using commercial SQUID magnetometer -- Indiana

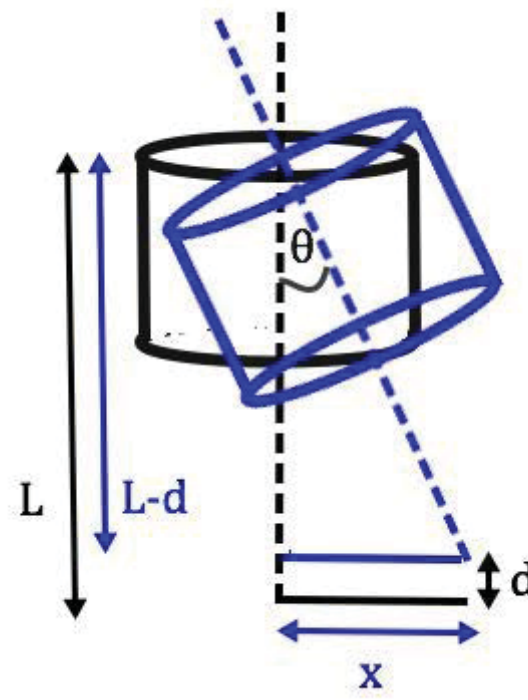


Magnetic impurities below 0.4 ppm

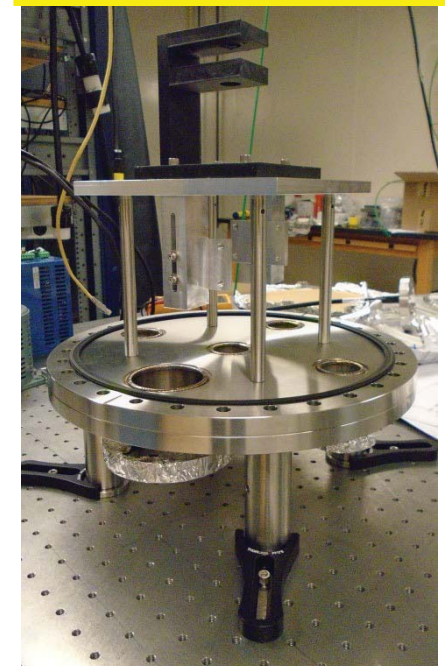
Rotary stage vibration and tilt



Interferometers

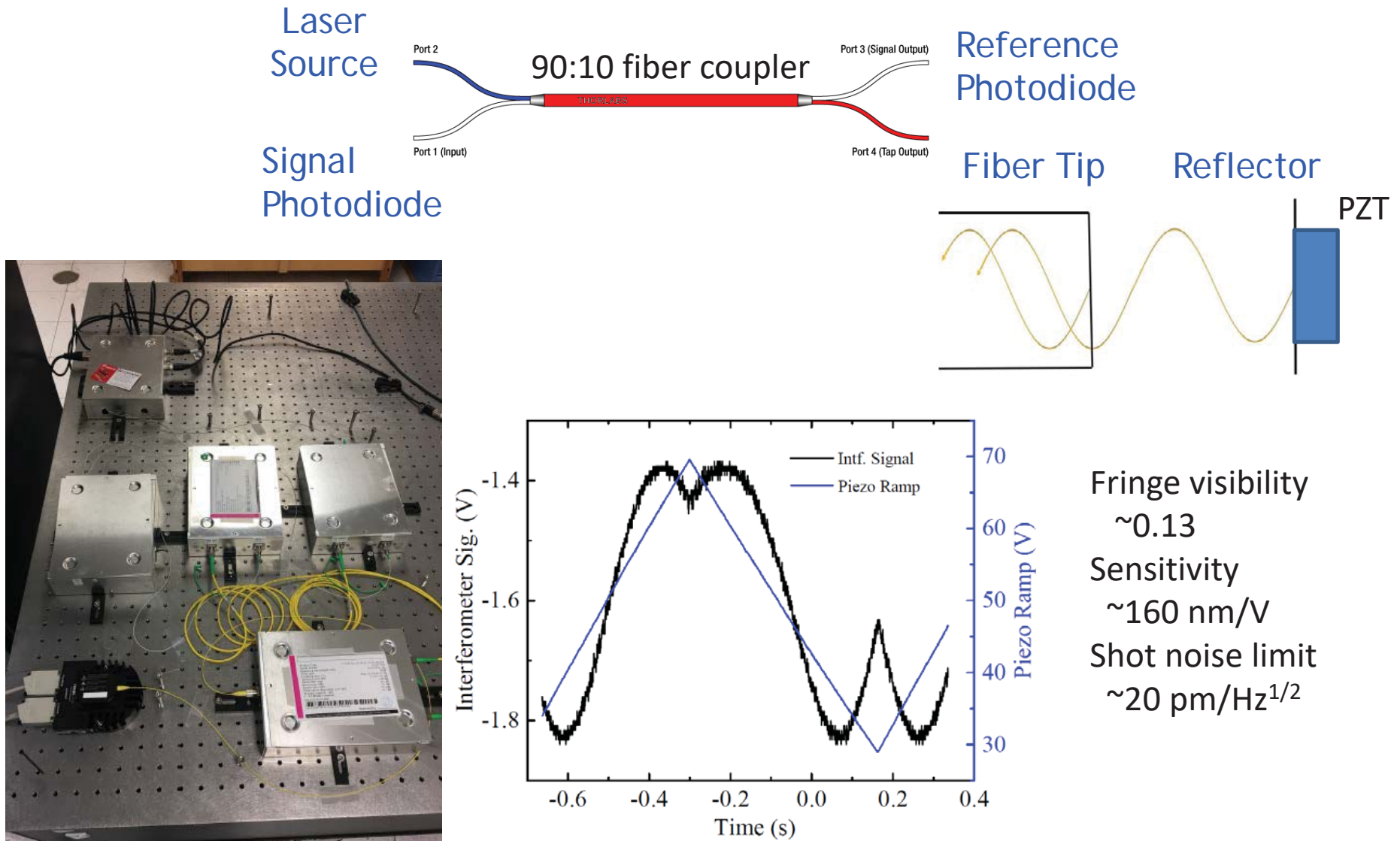


Rotary test chamber



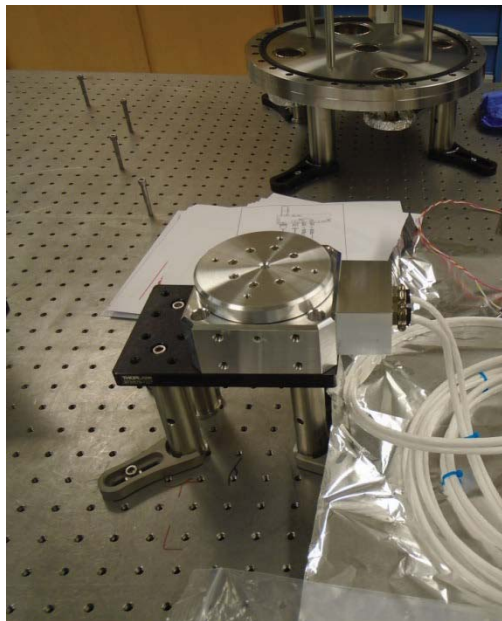
- Build an interferometer to measure the change in distance (d).
- We can find theta (Θ) from:
$$\Theta = \cos^{-1}((L-d)/L)$$
- We can solve for the wobble distance (X) by:
$$X = L\sin(\Theta)$$

Fiber-coupled laser interferometers

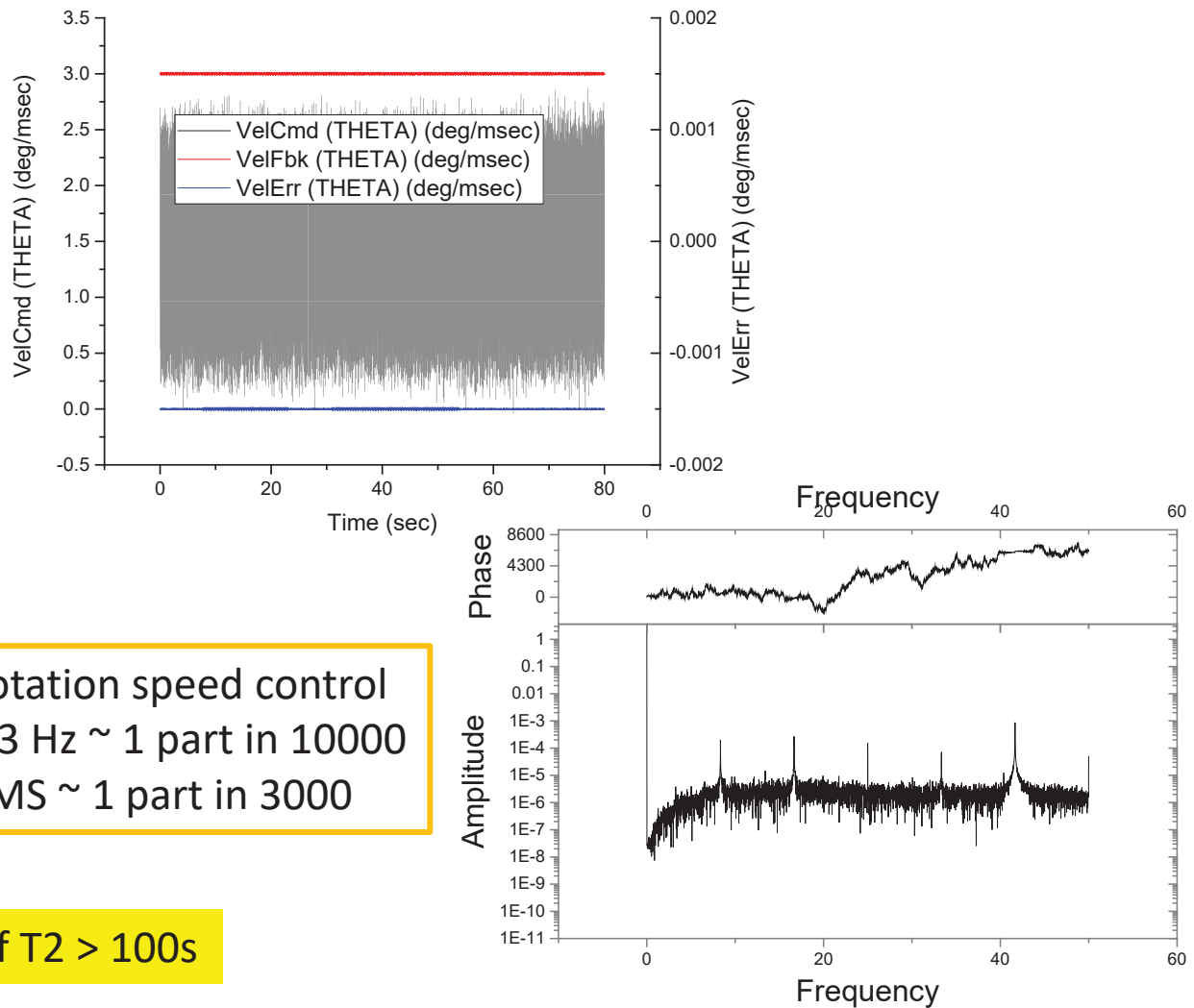


Speed stability test - direct drive stage

- Optical encoder
- Current feedback control



Stage speed stability error – unloaded, in air



Summary

- ARIADNE → New resonant NMR method
- Gap in experimental QCD axion searches
 $0.1 \text{ meV} < m_a < 10 \text{ meV}$
- Complementary to cavity-type (e.g. ADMX) experiments
- No need to scan mass, indep. of local DM density
- Next tests – shielding (Stanford/Korea), vibration (UNR), ${}^3\text{He}$ system (Indiana)



PHY-1205994
PHY-1506431
PHY-1506508
1510484, 1509176



Acknowledgements



University of Nevada, Reno



Back row (L to R): Cris Montoya (G), William Eom (UG), Jason Lim (UG), Harry Fosbinder-Elkins (UG), Mindy Harkness (UG), Andrew Geraci (PI)
Front row (L to R): Ryan Danenberg (UG), Kathleen Wright (UG), Isabella Rodriguez (UG), Chloe Lohmeyer (G), Ohidul Mojumder (UG), Jordan Dargert (G), Chethn Galla (G), Colin Bradley (UG).